

# Enhancing Pipeline Weldment Durability: Impact of Surface Area on Non-Elastic Performance Factors using RSM and ANN

<sup>1</sup>Mabiaku T.A., <sup>1</sup>Achebo J. I., <sup>2</sup>Obahiagbon K. O., <sup>1</sup>Ozigagun A., <sup>\*1</sup>Uwoghiren F. O.

Science and Engineering

<sup>1</sup>Department of Production Engineering, University of Benin, Benin City, +234, Nigeria.

<sup>2</sup>Department of Chemical Engineering, University of Benin, Benin City, +234, Nigeria.

E-mail: [timothy.mabiaku@gmail.com](mailto:timothy.mabiaku@gmail.com), [joseph.achebo@uniben.edu](mailto:joseph.achebo@uniben.edu), [kess.obahiagbon@uniben.edu](mailto:kess.obahiagbon@uniben.edu),  
[andrew.ozigagun@uniben.edu](mailto:andrew.ozigagun@uniben.edu), [frank.uwoghiren@uniben.edu](mailto:frank.uwoghiren@uniben.edu)

Corresponding author: Uwoghiren F.O.

Accepted: 17/7/2024

Published: 25/7/2024

**Abstract:** Pipeline networks are essential for moving a variety of gases and liquids throughout different industrial sectors. By examining the effects of a particular non-elastic factor—the surface area of contact—on pipeline weldments and how those effects interact with elastic qualities, the study seeks to close this gap. In order to achieve this goal, an extensive experimental investigation is carried out that includes a variety of welding techniques, materials, and ambient circumstances in order to faithfully mimic real-world scenarios. The central composite design, which was painstakingly created with the aid of design expert software (version 13.0), is followed by the experimental setup. The response surface approach study provides the best results, recommending a voltage of 21.280 volts, a current of 160.000 amps, and a gas flow rate of 14.667 liters per minute. With the combined use of these input parameters, a welded junction with a surface area value of 40.670 and an attractiveness value of 0.918 was produced. Furthermore, in order to forecast output parameters, the Artificial Neural Network model is utilized and contrasted with the Response Surface Methodology. The results highlight how important it is to optimize non-elastic performance variables for pipeline weldments. Weldments can be constructed to withstand harsh circumstances, reduce the likelihood of failures, and greatly extend the operating lifespan of pipelines by precisely managing the surface area of contact.

**Keywords:** pipeline weldments, surface area, input parameters, artificial neural network, response surface methodology.

Published by GJEST

## 1. INTRODUCTION

Weld integrity is a critical aspect of welding processes, ensuring the strength and reliability of welded joints (Song et al., 2022). The surface area of contact between the materials being welded is a fundamental factor that significantly affects the quality and integrity of the weld (Jabar et al., 2023). A larger surface area of contact generally leads to improved weld integrity due to enhanced heat transfer, better fusion, and reduced stress concentrations (Benedetti et al., 2021). This literature review explores the impact of surface area of contact on weld integrity, encompassing various welding processes and materials. In welding, the surface area of contact refers to the interface between two materials to be joined (McCrea et al., 2023). This area is essential in establishing the quality and strength of the resultant weld. Several factors influence the surface area of contact, including joint design, material thickness, and welding process (Davis et al., 2021). Joint design is a critical

consideration in welding processes (Singh & Shahi, 2018). The type of joint, such as butt, lap, or fillet, affects the surface area of contact (Sejani et al., 2022). For example, a butt joint provides a larger surface area of contact compared to a lap joint, leading to improved weld integrity. Research has shown that joint design optimization is essential for achieving the desired weld strength and integrity (Adame et al., 2022). Material thickness significantly impacts the surface area of contact (Liu et al., 2019). Thicker materials generally have larger surface areas, which can influence heat distribution during welding. It is essential to consider material thickness when determining welding parameters and procedures to ensure proper fusion and prevent defects (Vasilev et al., 2021). Different welding processes, including laser, resistance, and arc welding, have varying effects on the surface area of contact. For instance, Gas tungsten arc welding (GTAW) and gas metal arc welding (GMAW) are two examples of arc welding procedures that

can provide precise control over the surface area of contact due to their focused heat source (Gibson et al., 2021). A larger surface area allows for better heat distribution during welding, reducing the likelihood of overheating or underheating, which can lead to defects like cracking or incomplete fusion (Jabar et al., 2023). Welds with larger surface areas of contact distribute stress more evenly, minimizing stress concentrations that can weaken the weld and lead to premature failure (Geng et al., 2020). A greater surface area facilitates improved fusion between the base materials and the filler metal, resulting in a stronger and more durable weld (Ho & Kontopoulou, 2022).

Numerous research studies have investigated the relationship between surface area of contact and weld integrity. These studies often involve experimental setups to assess the mechanical properties, microstructure, and defect formation in welds with varying surface areas of contact (Derazkola & Simchi, 2018). The results consistently highlight the importance of optimizing the surface area to achieve robust welds. The surface area of contact varies depending on the welding process used. Different welding techniques create different contact geometries (Behrens et al., 2021). In butt welding, two materials with flat surfaces are joined along their edges. The surface area of contact in butt welds is relatively large, resulting in strong and reliable joints (Ye et al., 2018). These are commonly used in structural applications. Lap welding involves overlapping two materials, creating a smaller contact area. While lap welds are easier to perform, they may have reduced strength compared to butt welds (Inamke et al., 2019). Fillet welds are used in corner joints and have a triangular cross-section. The surface area of contact in fillet welds is smaller than that in butt welds, making them suitable for lighter loads (Yaghoubi & Tavakoli, 2022). Surface preparation is a critical step in welding that directly affects the surface area of contact. Proper surface preparation involves removing contaminants, oxides, and debris from the materials being joined. This ensures a clean and well-defined contact area, improving weld quality (Pang et al., 2023).

## 2. THEORETICAL ANALYSIS

In this research, a response surface methodology (RSM)-based attempt is made to construct a second order mathematical relationship between one response parameter, surface area, and several input factors, including voltage (V), current (I), and gas flow rate (GFR).

The objective of the optimization model was to raise the contact surface area.

The ideal number for every input variable, including the gas flow rate (l/min), voltage (Volt), and current (Amp), which will maximise surface area contact, was found to be the process' end outcome.

To generate the experimental data necessary for the optimisation procedure;

i. The central composite design approach (CCD) was employed for the statistical design of the experiment (DOE). A statistical program was used for the design and optimization procedures. In this particular case, it was decided to use Design Expert 7.01.

ii. The next stage was to create an experimental design matrix that contained eight factorial points ( $2n$ ), six axial points ( $2n$ ), and six center points ( $k$ ) for a total of twenty experimental runs.

### A. Response Surface Methodology

Engineers frequently employed Response Surface Methodology (RSM) to identify the ideal circumstances required to carry out a certain activity. Finding the input parameter values for a process that produce the optimal outcomes, whether they involve decreasing or maximizing a specific parameter, is required. By using mathematical and statistical techniques to model and forecast the intended response, RSM is a commonly utilized optimization methodology that aids engineers in understanding how a process functions. The goal is to maximize or optimize the use of this reaction, which is dependent on several input variables.

### B. Artificial Neural Network

An extremely parallel and distributed computer system called a neural network has the capacity to hold experimental data for a variety of purposes. It works as a tool for data mining and is primarily made to seek obscure trends within datasets. It's interesting to note that the human brain and neural networks have two important characteristics. First, synaptic weights are used to store knowledge throughout the network's process of learning. These weights represent the degree of connectivity between inner neurons. Second, the transfer function ( $f$ ) computes the sum of these weighted inputs coupled for every basic neuron with  $R$  inputs, there is a bias term and suitable weights ( $w$ ) applied. Any differentiable function that is used to predict the outcomes of neurons can be the transfer function ( $f$ ). The log-sigmoid transfer function, often known as  $\text{logsig}$ , is frequently used in multilayer networks. The output values of the sigmoid transfer function, and more precisely the log-sigmoid, range from 0 to 1, depending on whether the net input to the neuron is either negative or positive infinity. Some multilayer networks choose the tan-sigmoid transfer function, demonstrating the flexibility in transfer function selection. While sigmoid output neurons are usually preferred for challenges that involves trend recognition, linear output neurons are effective for addressing function-fitting concerns.

In summary, artificial neural networks are software-based data mining techniques that leverage principles of neuronal transmission, drawing inspiration from the functioning of the human brain. They function as predictive tools that analyze data using techniques like training, learning, validation, and testing to make accurate predictions and unearth insightful information.

### 3. MATERIALS AND METHODS/METHODOLOGY/EXPERIMENTAL PROCEDURE

#### A. Process parameters

Several factors were examined in this research study in connection to the welding pool's temperature. The welding current, voltage, and gas flow rate were among these factors. Twenty runs were made using different welding current, voltage, and gas flow rates to complete the trials, and these runs were utilized to join two mild steel plates that were each 60 x 40 x 10 mm in size. A specialized Brinell hardness testing unit was employed to conduct the Brinell hardness test in order to determine the hardness of the final welds. A ball made of tungsten carbide with a fixed diameter (D) is used in this test. A predetermined force (F) is applied to the ball, which is then held in position for a predetermined amount of time (T) before being released. This procedure causes the tested metal component to permanently distort or bear an imprint from the spherical indenter. By averaging measurements of the indentation's diameter taken from two or more places, the indentation's diameter (d) is established. A loading system made up of a hydraulic dashpot, weights, plunger, and levers surrounds the body of the Brinell hardness testing machine to carry out the test. Over on the moveable anvil is where the sample is placed. The ball-shaped indenter drops onto the sample when the lever is pulled, exerting a preset force that is subsequently displayed and examined on the display.

#### B. Design of experiment

A systematic and scientific process known as the design of experiments (DOE) is utilized to prepare and perform tests to determine a cause-and-effect relationship between variables. It is also a rigorous method for modifying a process' input variables and evaluating the outcomes while taking the process' intrinsic random unpredictability into account. Scientific research must include experimentation, and software programs like

Design Expert and Minitab greatly aid in making this process easier. These computer programs assist in data collection using experimental methods to guarantee accurate polynomial approximations. The Latin hypercube, full factorial, both the face-centered and the circumscribed central composite experimental designs are among the many types that are accessible. The amount of input parameters considered in this research, which developed models for all the responses using Design Expert software, had an impact on the choice of the central composite design for performing experiments.

#### C. Materials and experimental set-up

Thermocouples were mounted in the gas tungsten arc welding (GTAW) system, which worked in the current range of 150 to 200 A. A 200 x 200 x 20 mm<sup>3</sup> block of low-carbon steel underwent this welding procedure. The gas was shielded using a DCEN (Direct Current Electrode Negative) setup with a 4 mm-arc gap. Measurements of temperature were made between 1500 and 1800 °C. Due to their exceptional resilience to high temperatures, W5 tungsten thermocouples were employed. The tungsten wires and sleeving combined to give these thermocouples an overall diameter of 1.2 mm. They had a diameter of 1.4 mm, a 20° angle, and were introduced into the samples to a depth of 4 mm.

#### D. Method of Data Collection

Twenty test runs were conducted utilizing the central composite design matrix that the Design Expert software developed. The weld sample results, together with input and output parameters, were included in these test runs. The formula, denoted as Equation 2<sup>n</sup> + 2n + k, encompasses the following variables: k represents the count of center points, 2n signifies the quantity of axial points, and 2n pertains to the number of factorial points, was used to calculate the size of the data matrix. After that, this matrix was examined employing artificial neural networks (ANNs) with the Response Surface Methodology (RSM) techniques.

## 4. RESULTS AND DISCUSSION

To evaluate the appropriateness of the quadratic model for analyzing the experimental data, the sum of squares of the sequential model was computed particularly for the surface area response parameter. The results of this calculation are summarized in Table 2.

**Table 2:** Sequential model sum of square for surface area of weld

Source	Sum of Squares	df	Mean Square	F-value	p-value	
Mean vs Total	31134.73	1	31134.73			
Linear vs Mean	39.48	3	13.16	0.7095	0.5604	
2FI vs Linear	121.83	3	40.61	3.02	0.0683	
<b>Quadratic vs 2FI</b>	<b>170.97</b>	<b>3</b>	<b>56.99</b>	<b>143.83</b>	<b>&lt; 0.0001</b>	<b>Suggested</b>
Cubic vs Quadratic	3.75	4	0.9369	26.19	0.0006	Aliased
Residual	0.2147	6	0.0358			
Total	31470.97	20	1573.55			

The sequential model sum of squares table demonstrates how the model fits improves when more terms are introduced. Based on the calculated sequential model sum of squares, the highest order polynomial with significant extra terms and no aliasing was selected as the best fit. It was discovered that the cubic polynomial was aliased based on the results in table 2, hence it is not suitable for fitting the final model. Furthermore, the use of the quadratic polynomial in this study was supported by the suggestion that the quadratic and 2FI model better fit the data.

To assess the explanatory power of the quadratic model in capturing the inherent variation within the experimental findings, a test for lack of fit was carried out every one of the response variables. A model with a noticeable lack of fit is typically not suitable for making accurate predictions. Findings from the computed lack of fit test for the surface area of contact response are presented in Table 3.

**Table 3:** Lack of Fit Test for a Surface Area of Contact

Source	Sum of Squares	df	Mean Square	F-value	p-value	
Linear	296.76	11	26.98	6.25	0.0256	
2FI	174.93	8	21.87	8.37	0.0142	
Quadratic	3.96	5	0.7925	<b>0.6599</b>	<b>0.7311</b>	<b>Suggested</b>
Cubic	0.2147	1	0.2147	0.3939	0.6937	Aliased
Pure Error	0.0000	5	0.0000			

The model statistics for the surface area response, derived from various model sources, which are compiled in Table 4.

**Table 4:** Model Summary Statistics for Surface Area of Weld

Source	Std. Dev.	R <sup>2</sup>	Adjusted R <sup>2</sup>	Predicted R <sup>2</sup>	PRESS	
Linear	4.31	0.1174	-0.0481	-0.4946	502.53	
2FI	3.67	0.4797	0.2396	-0.1277	379.17	
<b>Quadratic</b>	<b>0.6295</b>	<b>0.9882</b>	<b>0.9776</b>	<b>0.9077</b>	<b>31.03</b>	<b>Suggested</b>
Cubic	0.1891	0.9994	0.9980	0.8593	47.32	Aliased

Each entire model's standard deviation, R-squared (R<sup>2</sup>), adjusted R-squared (Adjusted R<sup>2</sup>), predicted R-squared (Predicted R<sup>2</sup>), and Predicted Error Sum of Squares (PRESS) statistics are shown in the statistical analysis of model fit. Low PRESS, R-Squared around one, and a low standard deviation are the optimum parameters for locating the best model source,

comparatively. The quadratic polynomial model was selected for this study because, based on its findings presented in Table 4, it was evident that the cubic polynomial model exhibited aliasing.

Table 5's goodness of fit statistics are used to confirm that the quadratic model is adequate according to its ability to maximise surface area.

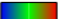
**Table 5:** GOF Statistics for Surface Area of Weld

<b>Std. Dev.</b>	0.6295	<b>R<sup>2</sup></b>	0.9882
<b>Mean</b>	39.46	<b>Adjusted R<sup>2</sup></b>	0.9776
<b>C.V. %</b>	1.60	<b>Predicted R<sup>2</sup></b>	0.9077
		<b>Adeq Precision</b>	27.6746

The Predicted R<sup>2</sup> value of 0.9077 closely aligns with the Adjusted R<sup>2</sup> value of 0.9776, with a difference of under 0.2. This indicates that the expected and adjusted R<sup>2</sup> values are in a decent agreement, suggesting that the model provides a good fit to the data. Furthermore, the Adeq Precision metric, in which the signal-to-noise ratio is measured, is a valuable indicator of model reliability. When a ratio exceeds 4, it is generally considered desirable, and in your case, the model exhibits a ratio of 27.675. This high Adeq Precision value indicates that the model offers an adequate signal-to-noise ratio, making it suitable for navigating the design space effectively.

The anticipated values and the actual values were compared in order to pinpoint values or groups of values that the model would not have been able to easily pinpoint. This comparison is shown with an emphasis on surface area in Figure 2. For every response, a Cook's distance plot was created in order to look for any possible outliers in the experimental results. Cook's distance computes the possible effect on the regression of removing a certain point. To rule out outliers, greater attention should be paid to points with abnormally high distance values in comparison to the others. Figure 3 displays the surface area Cook's distance plot.

#### surface area of weld

Color points by value of surface area of weld:  
34.88  46.98

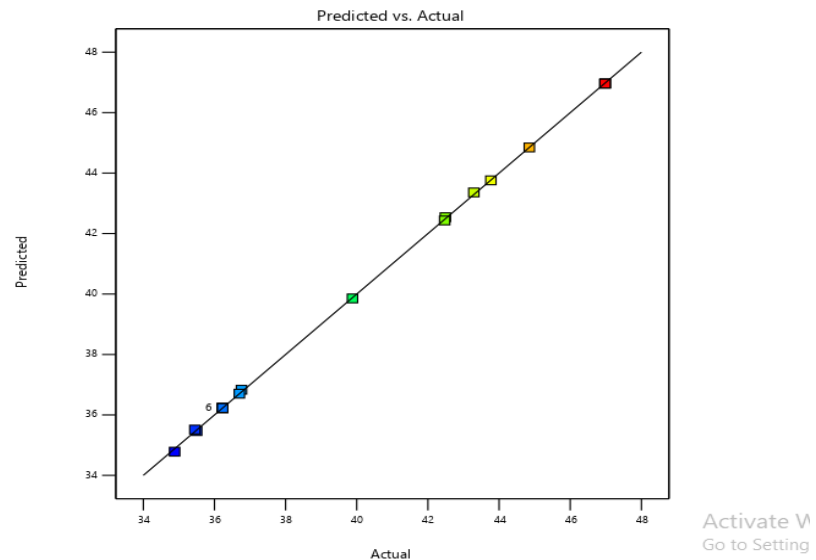
**Figure 2:** Plot of Predicted Vs Actual for surface area of weld

Figure 2 demonstrates how the dots are densely clustered close to the fitted line. This demonstrates that the model successfully estimates the majority of the data points. This is a sign that the forecast accuracy and inclination of the developed model are sufficient.

Figure 3A and 3B shows 3D surface plots analyse the impacts of voltage and current on the surface area. Figure

4A describes 3D surface plots were made to investigate the impacts of surface area on gas flow rate and current. The contour plots in Figure 4B illustrate the surface area of the weld response parameter in comparison to the ideal voltage and gas flow rate, as well as the 3D surface plots in Figure 6 were created to explore the impacts of voltage and gas flow rate on surface area.

surface area of weld (mm<sup>2</sup>)

● Design Points

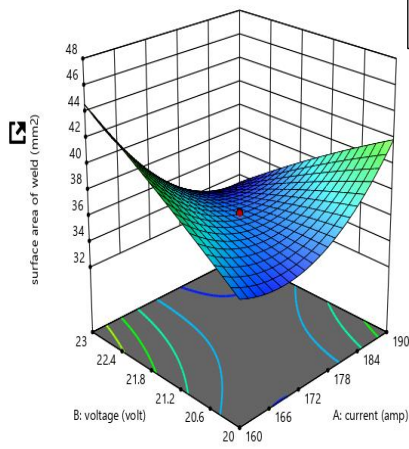
34.88 46.98

X1 = A

X2 = B

Actual Factor

C = 13.5



A

surface area of weld (mm<sup>2</sup>)

● Design Points

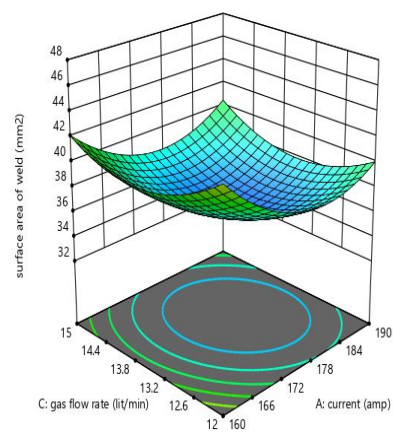
34.88 46.98

X1 = A

X2 = C

Actual Factor

B = 21.5



B

Figure 3: (A) Impact of voltage and current on surface area (B) Effect of gas flow rate and current on surface area

surface area of weld (mm<sup>2</sup>)

● Design Points

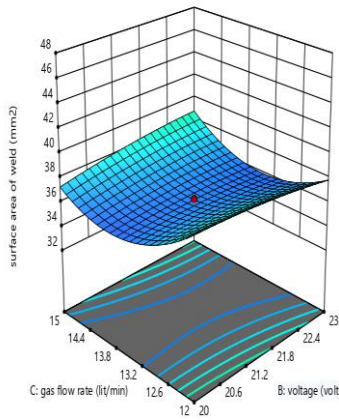
34.88 46.98

X1 = B

X2 = C

Actual Factor

A = 175



A

surface area of weld (mm<sup>2</sup>)

● Design Points

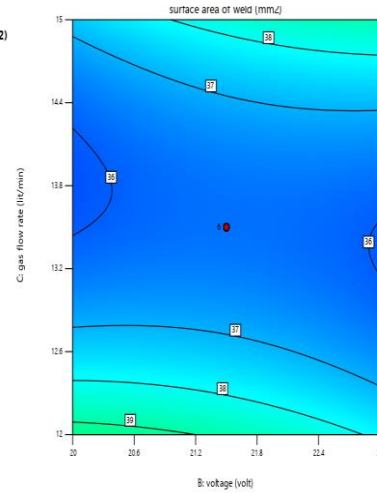
34.88 46.98

X1 = B

X2 = C

Actual Factor

A = 175



B

Figure 4 (A): Effect of voltage and gas flow rate on surface area of weld (B) Predicting surface area of weld using contour plot

### 3.2 Modelling and prediction using artificial neural network (ANN)

The analysis was useful in determining the exact mathematical connection between the output variable (surface area) and the input parameters (gas flow rate, voltage, and current). Two crucial factors were taken into consideration in the effort to achieve an ideal network layout that offers the best precision in understanding the relationship between the data's input and output. The initial component included choosing the most precise learning rule or training algorithm. Secondly, it was also thought about how many hidden neurons there might be in the network. Considering various factors, a range of training algorithms and varying number of hidden neurons were selected, and they were then exposed to experimental analysis. The primary aim was to pinpoint the optimal training algorithm and the most appropriate number of hidden neurons that, when employed together, result in the most precise and efficient network configuration. This decision-making procedure depended on the evaluation of  $R^2$  (coefficient of determination) and MSE (Mean Squared Error) values to assess model performance and accuracy. Regarding the Artificial Neural Network (ANN) analysis, MATLAB R2022a was the software of choice. To begin, the data was meticulously organized and stored within a dedicated folder in the MATLAB environment. Following this, a normalization procedure was applied, converting the data to a numeric matrix format. This normalization process automatically determined the dataset's range. Finally, the import function was used to seamlessly bring the data into the MATLAB environment, facilitating subsequent analysis and modelling tasks. The training approach for

Levenberg-Marquardt Back Propagation, known as the enhanced second-order gradient technique, has been determined as the most suitable learning rule and, as a result utilized in crafting the network structure. The Levenberg-Marquardt Back Propagation training algorithm was specifically set up with a network of twenty hidden neurons. There are one (1) output processing element and three (3) input processing elements (PEs) in this network. Twenty hidden neurons were chosen for each layer, and Mean Squared Error (MSE) and coefficients of determination ( $r^2$ ) were used to track the network's performance closely. The hyperbolic tangent (tan-sigmoid) transfer function was used by the input layer of this network architecture to determine the layer's output from the input data. The linear (purelin) transfer function was used in the output layer, on the other hand. The input data had to be split up into training, validation, and testing sets in order to create the network. To be more precise, 70% of the data was set aside for training, 15% for validation, and 15% for testing. A maximum of 1000 training epochs were used to assess the network's performance. The "trainlm" function was utilized for the training procedure, which changes the weight and bias parameters using the Levenberg-Marquardt optimization method. It is recognized that this function is among the fastest backpropagation algorithms available but does require relatively more memory compared to other alternatives. With three input variables, the surface area was then predicted using the same network design as a single response variable.

The back propagation neural network-generated network diagram for surface area prediction is shown in Figure 5 and follows the architecture of the Artificial Neural Network (3-20

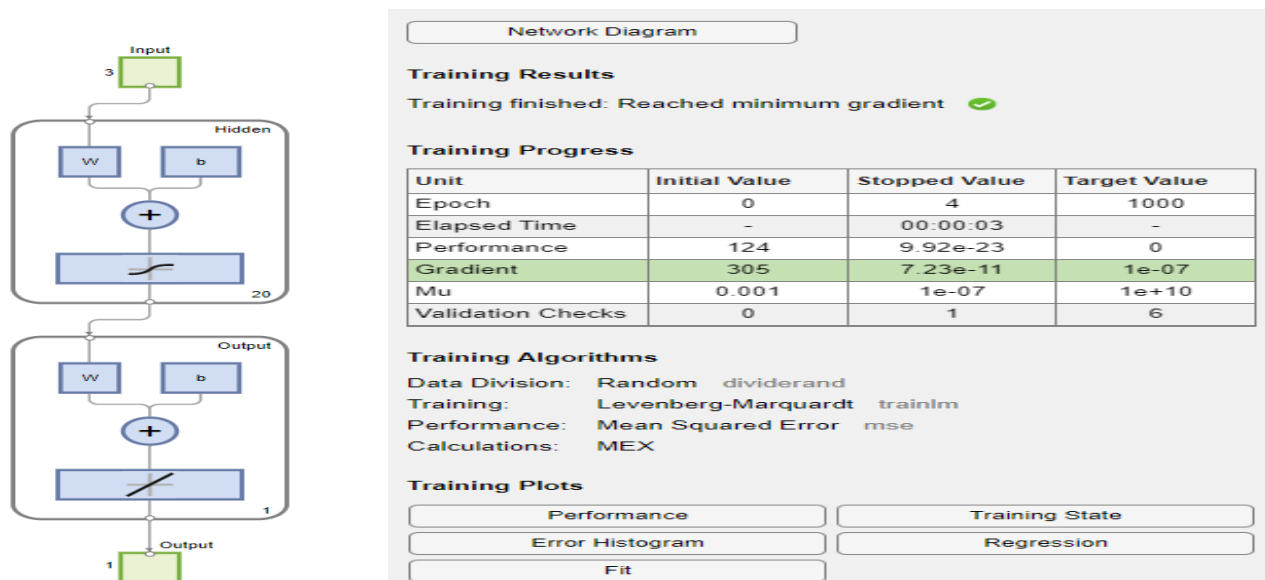
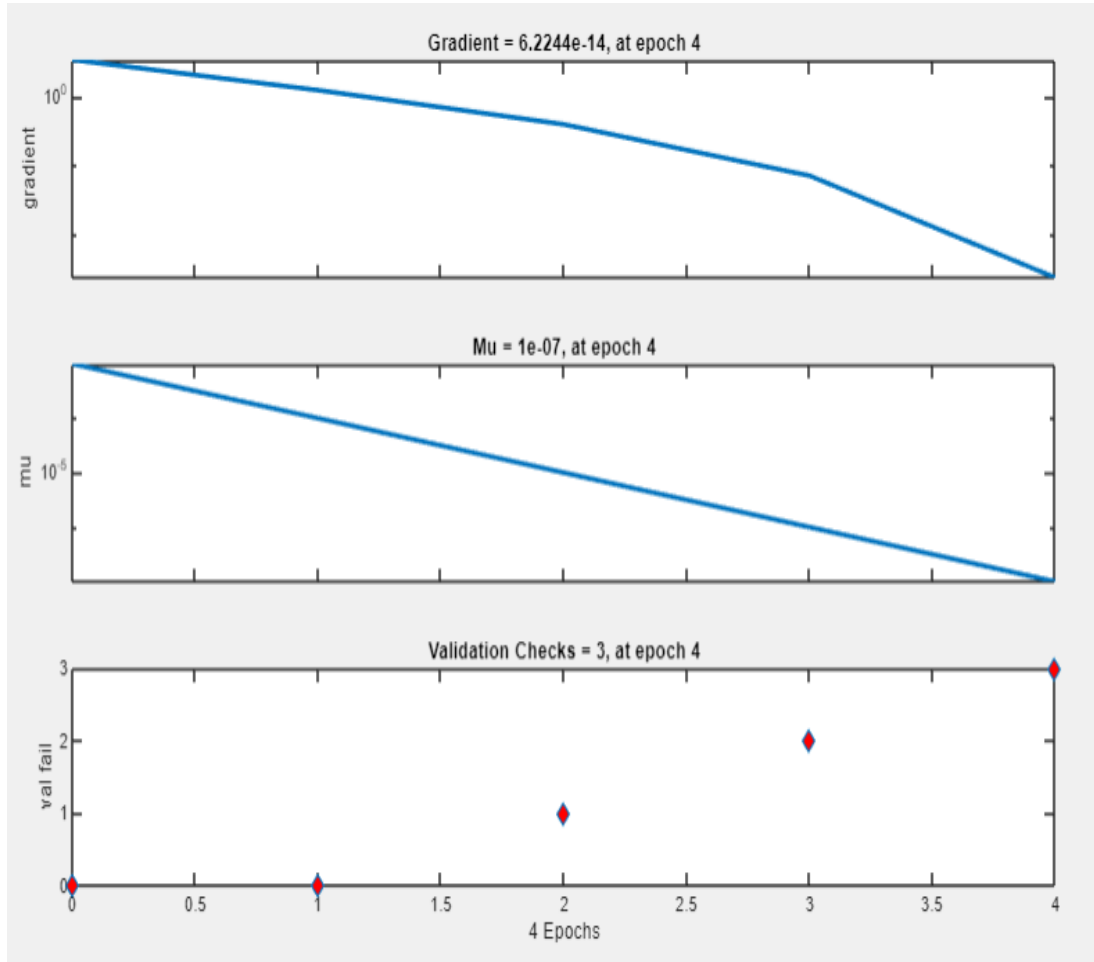


Figure 5: Model summary for predicting surface area

Based on the network training diagram shown in Figure 9, the network performance was found to be 124. One (1) observation was made out of six (6) validation checks. This is expected, though, since normalizing the raw data resolved the weight bias issue. Important

components such as the gradient function, training gain (Mu), and validation tests are shown in Figure 6, which also shows the training state. A full grasp of the training process and its associated components is made possible by this all-encompassing image.



**Figure 6:** Performance curve of trained network for predicting surface area

Backpropagation is a technique employed in artificial neural networks to assess the error impact of every neuron following a training batch of data. In essence, this process entails the neural network calculating the gradient of the loss function to elucidate the extent of mistake attributed to each of the chosen neurons. It's crucial to remember that a lower error value is more appealing. The computed gradient value of  $6.2244 \times 10^{-14}$ , as visualized in Figure 6, signifies that the chosen neurons' errors involvement are exceedingly minimal. Momentum gain (Mu) serves as an algorithmic control

parameter utilized in training the neural network. This parameter is essential to the training process and must adhere to a value less than unity. A momentum gain of  $1 \times 10^{-7}$ , as indicated here, is indicative of a network with substantial predictive capability, especially in relation to surface area. For further insight into the correlation between the input parameters (current, voltage, and gas flow rate) and the target parameter (surface area), as well as an overview of the training, validation, and testing progress, please refer to Figure 7, which presents a regression plot.



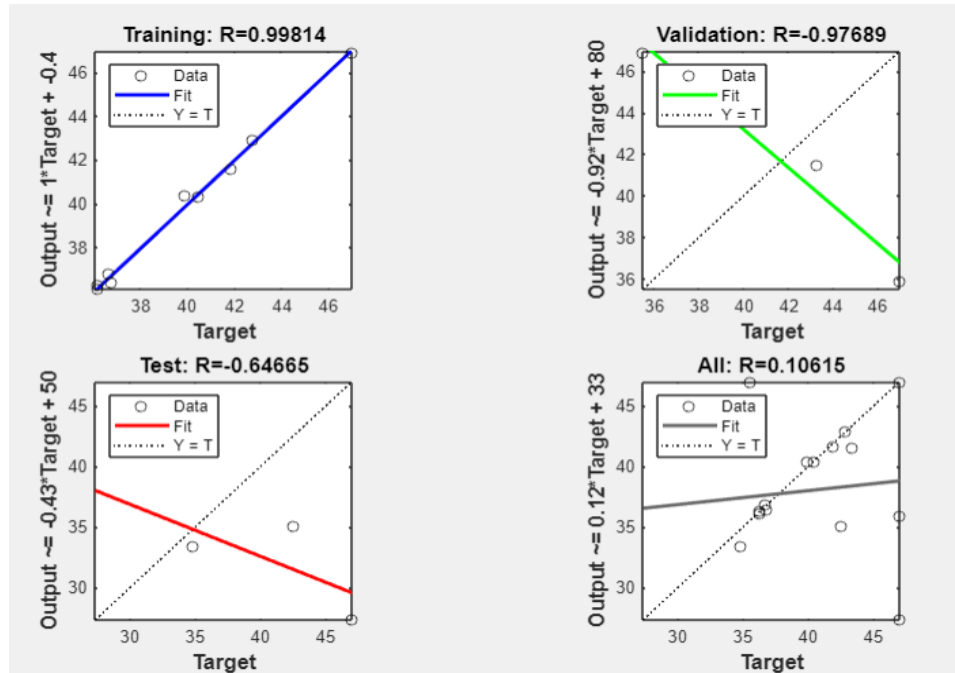


Figure 7: Regression plot showing the progress of training, validation and testing

## 5. CONCLUSION

In this research, the surface area of Tungsten inert gas-mild steel welds was optimized and predicted using the Response Surface approach and artificial neural network methods. The input parameters in this study encompass gas flow rate, voltage, and current, whereas the response parameter is the surface area of the weld. It's noteworthy that how these input parameters are related to one another and the corresponding responses is best described by a quadratic model. A sequential sum of squares test was used to make this conclusion, and the results indicated the significance of the quadratic model as seen by its incredibly low p-value ( 0.0001). Furthermore, when examining the model summary statistics across all the responses, it becomes evident that these models exhibit strong predictive capabilities. Each of them boasts an  $R^2$  value of approximately 90%, signifying the robustness and accuracy of the models in predicting outcomes. Additionally, it's noteworthy that these models do not exhibit a noticeable lack of fit, as evidenced by their p-values ( $> 0.005$ ). All together, the  $R^2$  values exceeding 0.9 emphasize the strength of these models and their effectiveness in predicting optimal values for the responses, particularly in the context of attaining welds of superior quality. Lastly, the variance inflation factor (VIF) value of 1.00 conforms to demands, further affirming the model's suitability for the analysis. According to the study, artificial neural networks can accurately predict the responses indicated above while

welding mild steel plates using tungsten inert gas. The experimental design was selected as the central composite design, which was generated by the design expert program (version 13.0). For a welded joint with a surface area of 40.670 and a desirability value of 0.918, the RSM analysis gave optimal solutions with current of 160.000 amps, voltage of 21.280 volts, and gas flow rate of 14.667 lit/min. The RSM methodology was contrasted with the artificial neural network model, which was used to project the parameters of the outcome. The Artificial Neural Network is chosen as the inferior prediction model derived from the results since it has a lower coefficient of determination than the response surface methodology.

## REFERENCES

- Adame, E.V.; Aleksa, A.; Gilbert, M.R.; Cuddy, M.; Calvet, T.; Vizvary, Z.; Mantel, N.; Maviglia, F. and You, J.H. (2022). Qualification and testing of joining development for DEMO limiter component. *Fusion Engineering and Design*, 180:113164.
- Behrens, B. A.; Uhe, J.; Petersen, T.; Nürnberger, F.; Kahra, C.; Ross, I. and Laeger, R. (2021). Contact geometry modification of friction-welded semi-finished products to improve the bonding of hybrid components. *Metals*, 11(1):115-126.

- Benedetti, M.; Du Plessis, A.; Ritchie, R. O.; Dallago, M.; Razavi, S. M. J. and Berto, F. (2021). Architected cellular materials: A review on their mechanical properties towards fatigue-tolerant design and fabrication. *Materials Science and Engineering: R: Reports*, 144, 100606.
- Davis, J.; Atmeh, M.; Barakat, N. and Ibrahim, A. (2021). Design and performance simulation of a triboelectric energy harvester for total hip replacement implants. In *Health Monitoring of Structural And Biological Systems XV*. SPIE. (11593):232-244
- Derazkola, H. A. and Simchi, A. (2018). Experimental and thermomechanical analysis of the effect of tool pin profile on the friction stir welding of poly (methyl methacrylate) sheets. *Journal of Manufacturing Processes*. (34): 412-423.
- Geng, P.; Qin, G. and Zhou, J. (2020). A computational modeling of fully friction contact-interaction in linear friction welding of Ni-based superalloys. *Materials & Design*. (185): 108244.
- Gibson, I.; Rosen, D.; Stucker, B.; Khorasani, M.; Gibson, I.; Rosen, D.; Stucker, B. and Khorasani, M. (2021). Directed energy deposition. *Additive Manufacturing Technologies*. 285-318.
- Ho, Q. B. and Kontopoulou, M. (2022). Improving the adhesion and properties in the material extrusion of polypropylene by blending with a polyolefin elastomer. *Additive Manufacturing*, 55, 102818.
- Inamke, G. V.; Pellone, L.; Ning, J. and Shin, Y. C. (2019). Enhancement of weld strength of laser-welded joints of AA6061-T6 and TZM alloys via novel dual-laser warm laser shock peening. *The International Journal of Advanced Manufacturing Technology*. (104): 907-919.
- Jabar, S.; Barenji, A. B.; Franciosa, P.; Kotadia, H. R. and Ceglarek, D. (2023). Effects of the adjustable ring-mode laser on intermetallic formation and mechanical properties of steel to aluminium laser welded lap joints. *Materials & Design*. (227):111774.
- Liu, J.; Zhang, Y.; Zhang, L.; Xie, F.; Vasileff, A. and Qiao, S. Z. (2019). Graphitic carbon nitride (g-C<sub>3</sub>N<sub>4</sub>)-derived N-rich graphene with tuneable interlayer distance as a high-rate anode for sodium-ion batteries. *Advanced Materials*, 31(24): 1901261.
- McCrea, J.; Palumbo, G.; Tomantschger, K. and Limoges, D. L. (2023). U.S. Patent Application No. 18/101,835.
- Pang, M.; Li, J.; Al\_Tamimi, H. M.; Elkamchouchi, D. H.; Ponnore, J. J. and Ali, H. E. (2023). Development of hybrid ANFIS-GAN-XGBOOST models for accurate prediction of material removal rates from PCB-polluted concrete surfaces using laser technology for sustainable energy generation. *Advances in Engineering Software*. (184):103500.
- Sejani, D.; Li, W. and Patel, V. (2022). Stationary shoulder friction stir welding–low heat input joining technique: a review in comparison with conventional FSW and bobbin tool FSW. *Critical Reviews in Solid State and Materials Sciences*, 47(6):865-914.
- Singh, J. and Shahi, A. S. (2018). Weld joint design and thermal aging influence on the metallurgical, sensitization and pitting corrosion behavior of AISI 304L stainless steel welds. *Journal of Manufacturing Processes*. (33):126-135.
- Song, W.; Liu, X.; Wang, P.; Liu, Y. and Berto, F. (2022). Strength mismatch effect on residual stress of 10CrNi3MoV steel considering the back-chipping process. *International Journal of Pressure Vessels and Piping*, (195):104570.
- Vasilev, M.; MacLeod, C.; Javadi, Y.; Pierce, G. and Gachagan, A. (2021). Feed forward control of welding process parameters through on-line ultrasonic thickness measurement. *Journal of Manufacturing Processes*, (64): 576-584.
- Yaghoubi, M. and Tavakoli, H. (2022). *Welded Joints*. In *Mechanical Design of Machine Elements by Graphical Methods* Cham: Springer International Publishing. 21-34.
- Ye, G.; Guo, J.; Sun, Z.; Li, C. and Zhong, S. (2018). Weld bead recognition using laser vision with model-based classification. *Robotics and Computer-Integrated Manufacturing*. (52): 9-16.